DOI: 10.1590/2317-4889201720170006

ARTICLE

# Application of persistent scatterers interferometry for surface displacements monitoring in N5E open pit iron mine using TerraSAR-X data, in Carajás Province, Amazon region

## *Aplicação de interferometria por espalhadores persistentes para monitoramento de deformações de superfície na mina de ferro a céu aberto N5E utilizando dados TerraSAR-X, na Província Carajás, região amazônica*

**Filipe Altoé Temporim[1]*, Fábio Furlan Gama[1], José Cláudio Mura[1], Waldir Renato Paradella[1], Guilherme Gregório Silva[1]**

**ABSTRACT:** Carajás Mineral Province, Amazon region, is the most important one in Brazil. Vale S.A. Company has the right to operate in the area of the N5E mine. The work is conducted on rock alteration products of low geomechanical quality related to sandstones, siltstones, and a lateritic cover. In order to monitor ground deformation, 33 TerraSAR-X images covering the period of March 2012–April 2013 were used in the investigation. An interferometric synthetic aperture radar (InSAR) approach based on permanent scatterer interferometry (PSI) using an interferometric point target analysis algorithm was applied. Results demonstrated that most of the area was considered stable during the time span of the image acquisition. However, persistent scatterers (PSs) with high deformation rates were mapped over a landfill probably related to settlements. To validate the PSI data, graphs were generated with the displaced information based on topographic measurements in the field. The graphs showed that the surface deformations during TSX-1 runway coverage are within the miner's safety threshold and do not present a risk of major problems. The PSI data provided a synoptic and detailed view of the deformation process that affects the mining complex without the need of field campaign or instrumentation.

**KEYWORDS:** TerraSAR-X; interferometry; Amazon; deformation; radar.

**RESUMO:** *A Província Mineral de Carajás, região amazônica, é a mais importante do Brasil. A Vale S.A. tem o direito de operar na área da mina N5E, que é conduzida em produtos de alteração de rochas de baixa qualidade geomecânica relacionados a arenitos, siltitos e uma cobertura laterítica. Para monitorar a deformação do solo, foram utilizadas 33 imagens de TerraSAR-X cobrindo o período de março de 2012 a abril de 2013. Foi aplicada uma abordagem interferométrica de radar de abertura sintética (InSAR) baseada em interferometria de espalhadores persistentes (PSI) utilizando um algoritmo de análise de alvo pontual. Os resultados mostraram que a maior parte da área foi considerada estável durante o período de aquisição de imagens, entretanto os espalhadores persistentes (PSs) com altas taxas de deformação foram mapeados em aterro, provavelmente relacionado a assentamentos. Para validar os dados PSI, foram gerados gráficos com os dados de deslocamento medidos em campo. Os gráficos mostraram que as deformações superficiais durante a cobertura das imagens TSX-1 estão conforme o limiar de segurança do minerador e não apresentam risco de problemas maiores. Os dados PSI forneceram uma visão sinóptica e detalhada do processo de deformação que afeta o complexo de mineração sem a necessidade de campanha de campo ou instrumentação.*

**PALAVRAS-CHAVE:** *TerraSAR-X; interferometria; Amazônia; deformação; radar.*

[1]National Institute for Space Research – INPE, São José dos Campos (SP), Brazil. *E-mails*: filipetemporim@gmail.com; fabio@dpi.inpe.br, mura@dpi.inpe.br, waldir@dsr.inpe.br, guilherme.gregorio@inpe.br

*Corresponding author.

**Manuscript ID:** 20170006. **Received in:** 01/16/2017. **Approved in:** 04/18/2017.

This work was supported by the [FAPESP – Foundation for Research Support of the State of São Paulo] under Grant [number 2010/51267-9].

## INTRODUCTION

The Brazilian mining industry is very diverse, with at least 55 mineral commodities currently explored in the country (DNPM 2015). The Mining Production Index (MPI), which measures the change in the quantity produced, grew 15.5% in the first half of 2015, if compared to the same period in the previous year. This performance was achieved mainly due to increased amounts of copper, manganese and iron (DNPM 2015).

Operations in open pit mines normally occupy large areas, including adjacent land portions of the pit. According to Stacey and Read (2009), instabilities can occur in these areas due to the mass movement of rocks and soils, steep slope of the mine stands, torrential rains and other factors that occur at regular mining operations. This scenario becomes worse in the Amazon region due to deep excavation in soils and saprolites with low geomechanical quality along with blasting practices and intense precipitation, with negative effects on the overall stability (Paradella *et al*. 2015).

According to Brito (2011), the main element of an open pit mine is the slope of benches. The geology of the deposit defines the area coverage and the depth of the mine pit, whereas the geotechnical characteristics define the steepness that the ore can be excavated. Mining benches are designed with safety factors to control the risks to personnel and equipment from possible instabilities. However, due to its need to obtain the highest possible economic gains, the ore exploitation involves the final slope increasingly steep by decreasing the removal of waste material. Taking these aspects, the surface deformation on information and slope stability are important items in the mining industry, for legal reasons, security, planning and production.

Currently, the most commonly used field surface displacement monitoring methods are optical leveling, total station reflective prisms or Global Positioning System (GPS) (Vaziri, Moore and Ali 2010). These types of survey provide updated information with sub-millimetric to centimetric resolution from localized areas. However, radar imaging systems based on Synthetic Aperture Radar (SAR) are capable of operating in all weather conditions and collect data, both during the day and at night, particularly orbital systems, which provide a synoptic vision of the area without the need for ground instrumentation and field campaigns (Ng *et al*. 2011). The integration of SAR imaging techniques, geographic information systems (GIS) and geotechnical measurements to monitor surface subsidence induced by mining as a complementary tool to traditional survey methods was discussed by Ge, Chang and Rizos (2007) and Ng *et al*. (2009). An integration of SAR techniques to monitor distinct displacements regimes (small to high deformation rates) was proposed by Paradella *et al*. (2015).

The interferometry technique using Synthetic Aperture Radar (InSAR) is based on a combination of two SAR complex images (SLC) acquired over the same area with a somewhat different acquisition geometries to ensure a phase difference (interference) between the scenes (Zebker and Villasenor, 1992). With this approach, it is possible to extract surface displacement along the Line of Sight (LoS) of the SAR for common pixels in the same position on the ground. However, this technique is only possible in areas with good interferometric coherence spatially distributed (as low vegetated terrain).

The technique of Permanent Scatterer Interferometry (PSInSAR) was proposed by Ferretti, Prati and Rocca (2000) and deals with the identification and monitoring of a point-wise persistent scatter (PS), pixels that show stable amplitude and coherent phase throughout a temporal sequence of images. PS have stable backscatter like structures built by man (street poles, transmission towers, buildings, bridges, exposed pipelines, roof, objects that are associated with dihedral of trihedrons responses) and natural targets (rock outcrops, soils and not vegetated surfaces etc.). A minimum of 15 images (stack) is used, and the accuracy of the deformation detected in this time series is of the order of a few millimeters per year on the imaging LoS. Current studies demonstrate the effectiveness of this technique when applied to the monitoring of surface deformation, as present by Gama *et al*. (2013), Pinto *et al*. (2015), and Costantini *et al*. (2016). In this paper, we present the results of the application of interferometry persistent scatterer (PSI) for surface displacement mapping in N5E iron mine, using TerraSAR-X (TSX-1) data.

## STUDY AREA

The Carajás Mineral Province (CMP) is the most important of Brazil and includes the largest iron deposits in the world; it is located on the eastern border of the Amazon, in the state of Pará. It covers an area of 120,000 km$^2$ and is marked by mountainous terrain, characterized by a set of hills and plateaus (altitude 500–900 m), surrounded by plains to the south and north (altitude around 200 m), with deep chemical weathering, which produced thick layer of latosols, fully covered by tropical forest communities of Ombrophilous Equatorial species (Paradella *et al*. 1994). Belonging to the mining company Vale S.A., the operation in Carajás is performed using state of the art in the open mine benching. Current exploitation activities are related to two bodies of iron ore (N4 and N5), and the study area

is one of the four active mines, located on the easternmost part of the N5 iron ore, as shown in Figure 1.

The CMP is considered the largest one in Brazil and includes significant iron deposits (e.g., N4, N5), Cu (e.g., Salobo, Sossego, Serra Verde), Au (e.g., Serra Pelada), Mn (e.g., Azul, Buritirama) and Ni (e.g., Vermelho, Onça Puma). The CMP is part of an Archean block (> 2.5 Ga) in the southeastern portion of the Amazonian Craton. Its northern domain corresponds to the Carajás rift affected by the E–W trending Archean Itacaiunas Shear Belt (ISB). The ISB is characterized by two lithostructural domains: a set of imbricated ductile oblique thrusts in the southern sector and two strike-slip systems (Carajás and Cinzento) in the northern sector, according to Holdsworth and Pinheiro (2000) and Veneziani, Santos and Paradella (2004). The Carajás strike-slip system is the largest fault system recognized within the ISB.

The N5E mine falls within the domain of Parauapebas and Carajás Formations (Beisiegel *et al.* 1973, Meireles *et al.* 1984). Parauapebas Formation consists of metavolcanic rocks (metabasalts and metadiabases) with a high degree of weathering, forming clayey to earthy saprolite packages. In the field nomenclature, they were differentiated into "Weathered Mafic" (WM), "Semiweathered Mafic" (SWM) and "Unweathered Mafic" (UM), and include the iron formations in the south, north, east and west portions of the mine. The rocks show features of ductile and brittle deformations (shear event).

The ironstones of the Carajás Formation are characterized by hematites (HM). They are distinguished by bodies of soft hematite (laminated and powdery hematite); as well as by outcrops of hard hematite (HD) with plates of compact hematite with 5 cm thickness, interleaved with soft hematite (SH), and low content iron ore. In the study area, HD occurs in the central portion, while SH crops out as small lenses in the northwest portion of the mine oriented to NE-SW and NW-SE, which are the main shear directions. These units are covered by layered iron duricrusts and lateritic soils. The ore duricrust (OD) is characterized by having high iron content and consists of hematitic blocks cemented by hydrated iron oxide. Chemical duricrust (QD) has low iron content and is normally overlying mafic rocks cemented by goethite. Finally, basic dykes and

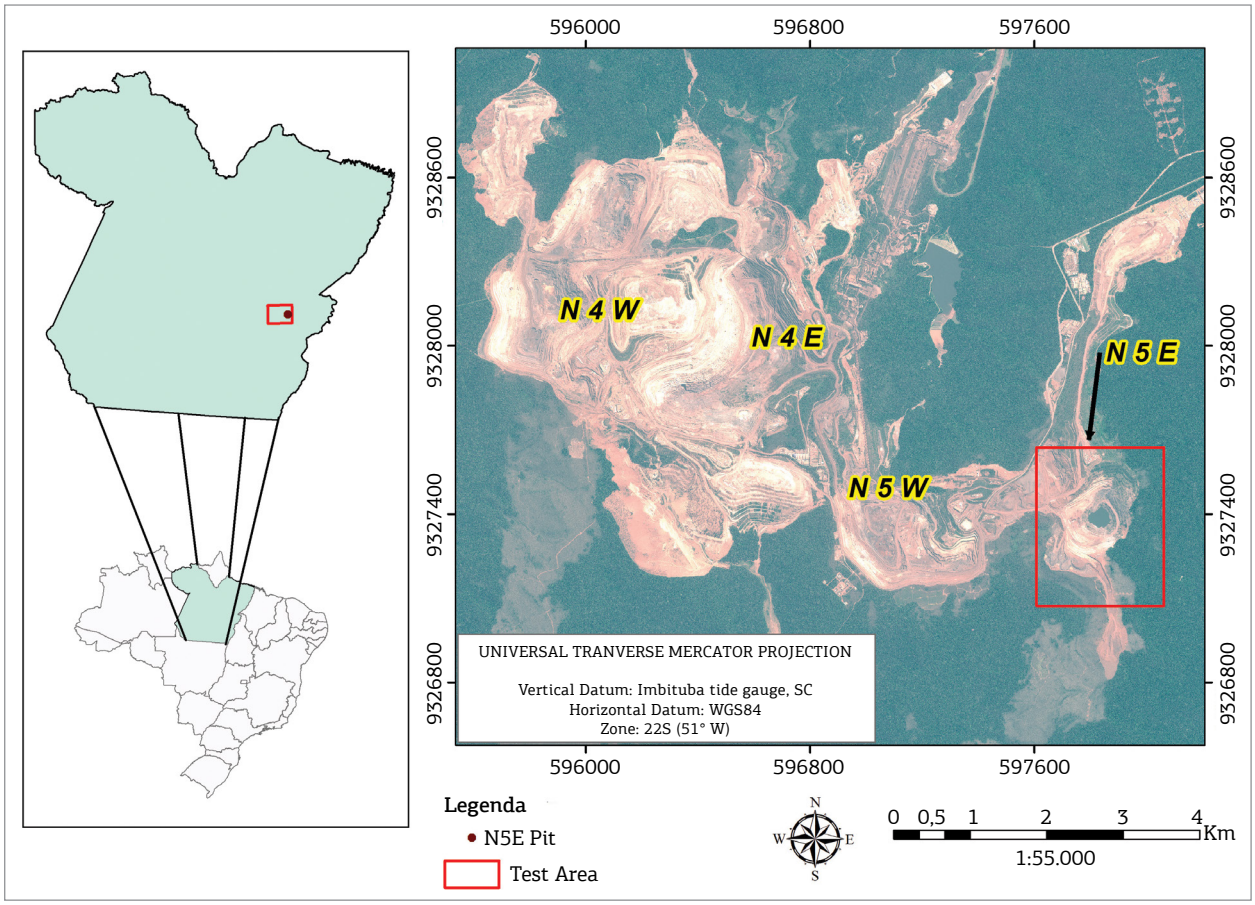


**Figure 1. Location of the study area (N5E mine).**

sills affected by low metamorphic grade are also mapped. The most detailed available account of the geological and geomechanical information for the N5E mine was produced by BVP Engineering (BVP 2011), including surface outcrop mapping at a 1:2000 scale, presented in Figure 2.

## DATASET

A stack with 33 TSX-1 StripMap images acquired during March 20, 2012 until April 07, 2013 was used in this paper. The single look complex (SLC) images were acquired under ascending passes (look azimuth 78 deg), incidence angle range of 39.89 to 42.21 deg, spatial resolution of 1.7 × 3.49 m (rg × az), pixel spacing of 1.36 × 1.90 m (rg × az), and width swath of 30 km. In order to minimize the topography phase error in the interferometric process, a high-resolution digital elevation model (DEM) was produced from a panchromatic GeoEye-1 stereo-pair acquired over the study area on July 1, 2012, with a vertical accuracy of 1.5 m (Paradella and Cheng, 2013).

## METHODOLOGICAL APPROACH

The pluviometric record during the TSX-1 passes was provided by the Vale S.A company. It indicated a total of 3,149 mm for cumulative precipitation. The dry season encompassed the interval from the end of March 2012 up to the beginning of October 2012, whereas the rainy season covered the period from October 2012 up to April 2013. Taking into account these values and the probable influence of rainfall in the SAR coherence, the PSI analysis was conducted in two stages: a first step using the first 19 TSX-1 images related to the dry season (March 20 to October 4, 2012); and a second step based on the last 15 TSX-1 scenes covering the wet season (October 4, 2012 to April 20, 2013).

The PSI technique is based on a series of differential interferograms, in which it is sought to identify spreaders targets whose dispersion properties vary little with time and angle of view, allowing a temporal analysis of the interferometric phase of individual points. Besides, it provides precise information related to the displacements of the surface in question. These highly coherent targets, PSs, identified in multiple

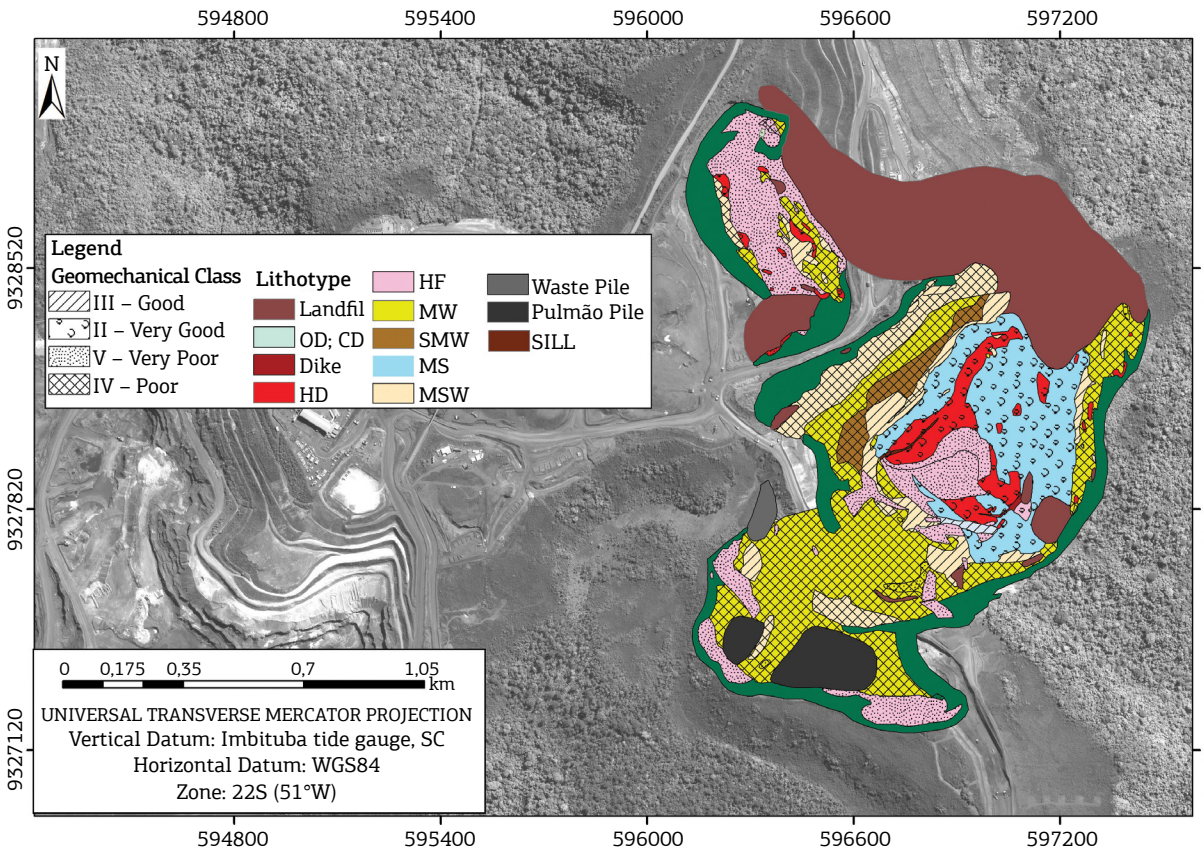


Acronyms: OD: ore duricrust; CD: chemical duricrust; HD: hard hematite; HF: lamellar hematite; MW: mafic weathered; SMW: superior mafic weathered; IMW: inferior mafic weathered; MSW: mafic semiweathered; MS: mafic shan.

**Figure 2. Lithological and geomechanical units in N5E mine.**

interferograms, allow to minimize and solve some of the problems related to the processing and the phase unwrapping, as well as a better discretization of the signals that occur in the interferometric phase, in addition to allowing the estimation and removal of orbital errors, and topography phase, deformation and atmosphere effects of the interferogram phase values, through their different behaviors in time and space (Ferretti, Prati and Rocca 2001, Werner *et al.* 2003; Hooper *et al.* 2004).

The Interferometric Point Target Analysis (IPTA), implementation of the PSI at the Gamma Remote Sensing software (Werner *et al.* 2003), was used to estimate the deformation vector ($Ø_{def}$) of each PS point, represented in equation Eq. 1, and consists in exploring some characteristics of the phase components, aiming at the separation or attenuation of each one of them.

$$\begin{aligned} D Ø_{PSj} &= Ø_{PSj\_def} + Ø_{psj\_eh} + Ø_{PSj\_atm} + Ø_{PSj\_noise} \\ D Ø_{j,1} &= Ø_{def\_1} + Ø_{eh\_1} + Ø_{atm\_1} + Ø_{noise\_1} \\ D Ø_{j,2} &= Ø_{def\_2} + Ø_{eh\_2} + Ø_{atm\_2} + Ø_{noise\_2} \\ &\vdots \\ D Ø_{j,M} &= Ø_{def\_M} + Ø_{eh\_M} + Ø_{atm\_1M} + Ø_{noise\_M} \end{aligned} \quad (1)$$

The processing initially consisted in generating a stack of images registered in the SLC format, for the construction of interferometric pairs. As shown in Figure 3, in the PSI approach a reference image (master image) was selected for the construction of interferometric pairs. This image was chosen based on a configuration that presents low perpendicular baseline diversity values and close to the temporal center of the image sequence, to ensure good interferometric coherence between the pairs. Following the processing, the phases corresponding to the topography extracted from the DEM were subtracted from the interferogram stack, resulting in a new stack of differential interferograms in relation to a selected stable reference point in the image coverage area. An important step in the PSI methodology is the identification of the persistent return points, which consists of consistent and stable point locations over a long period of time to allow the historical analysis of the phase.

The IPTA software is based on a two-dimensional regression model, since there is a linear dependence of the topographic phase with the perpendicular baseline, and also a linear dependence of the deformation with time is assumed. The deformation linear regression residuals contain the phase components related to the atmospheric phase as well as the

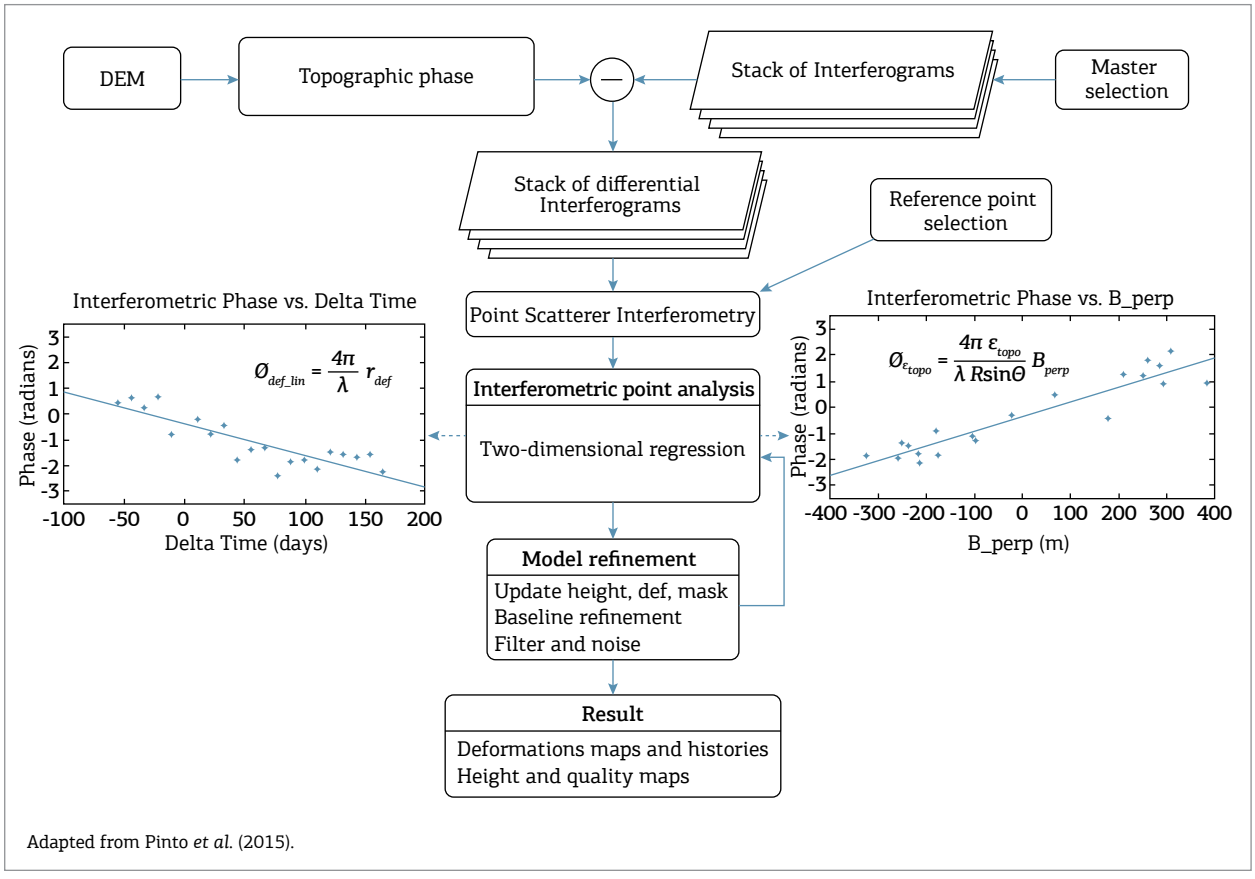


**Figure 3. Flowchart of the IPTA processing.**

phase components related to the nonlinear deformations and noise. These residues are spatially filtered to minimize the atmospheric phase as well as the phase noise, enabling the recovery of the phase component related to the nonlinear deformation. The PSI analysis is performed for all persistent return points, allowing the generation of a deformation map of the work area, as well as a map of the quality of each analyzed point.

## RESULTS AND DISCUSSIONS

Surface deformations at each PS position were expressed in terms of displacement rate and PSs were detected in relation to a reference point (coordinate 596148,449E; 9328050,899N of the World Geodetic System 84). The positive values, which correspond to the cold colors, indicate movement towards the satellite (uplift), while the negative values, pertaining to the warm colors, indicate the movement away from the satellite (subsidence).

The IPTA analysis for the dry season allowed the detection of 24,466 PSs in an area of 12.6 km$^2$, with an average density of ~ 1.942 PS/km$^2$. The use of the data stack for the wet season allowed the detection of 14,297 PSs, with an average density of ~ 1.135 PS/km$^2$. The deformation maps for both periods can be seen in Figure 4. There is a large difference in the number of points in relation to the two sets of images, due to the amount of rain in the wet season, which increases the temporal decorrelation due to the alteration of the dielectric constant of the targets, reducing the interferometric coherence. The PSs distribution was not homogeneous, since there was no PSs in vegetation areas (low coherence), while detection was very good in the mining areas (including the pit, processing facilities and related mining infrastructures). The IPTA results provided a synoptic view of the ongoing deformation process in the mining area and showed that most of the investigated site was stable during the TSX-1 coverage period (yellow-green regions in the maps of Fig. 4). The coherence loss of these sites can be caused by:

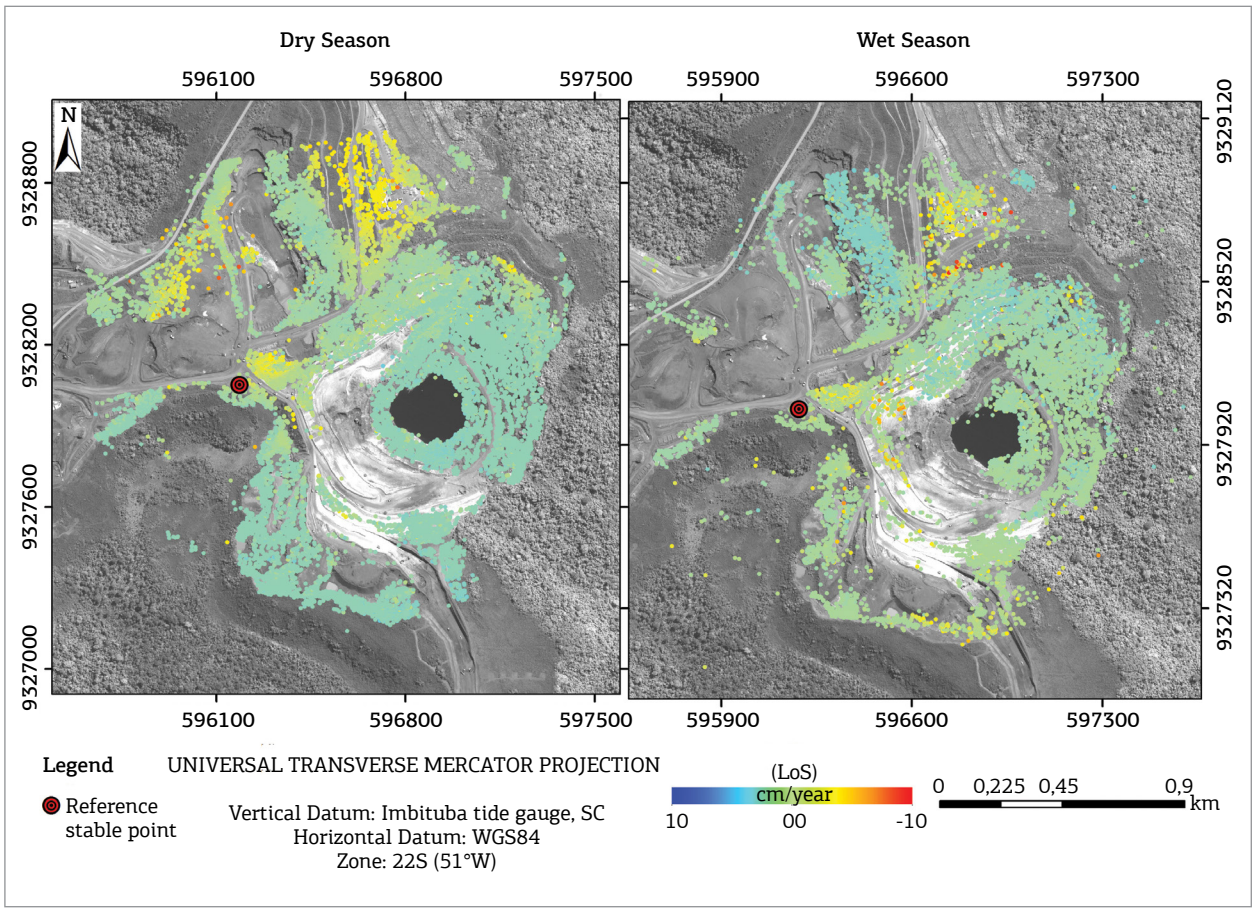


**Figure 4. Spatial distribution of persistent scatterers (PS) for N5E mine, visualized by the average line of sight (LoS) velocity on the panchromatic GeoEye-1 scene for dry and wet seasons. The reference stable point is shown in both set of images.**

- intense surface movement due to the mining processes;
- deformation occurring at a very high rate, beyond the sensitivity limit of the technique that is λ/4 (λ equals to 3,1 cm);
- influence of precipitation, particularly in the rainy season, with a change in backscattering characteristics.

For the areas around the mines, the lack of coherence is mainly associated with the presence of vegetation.

The accumulated values obtained in LoS that express subsidence are within the limits expected for an open pit operation of this size. The highest subsidence displacement values were identified north of the pit, in an area geologically mapped as a landfill, which justifies a greater displacement due to material accommodation over time. The maximum values of displacement rate at the landfill reached -94.92 mm during the dry season (March 20, 2012 until October 4, 2012) and -118.76 mm for the rainy season (October 4, 2012 until April 20, 2013). These values were negative, corresponding to the reddish spots in Figure 4, and therefore are indicative of subsidence. However, it is important to mention that, for the landfill, displacement with positive value expressing motion toward the satellite characterized by bulging at the dump toe indicative of terrain instabilities was not detected.

There is a general absence of PSs on the benches of the pit on the left side, as this synthetic structure underwent intense surface changes due to the ongoing mining operation, expressed by the low coherence. Another important fact that may be responsible by this lack of PSs at this site in both set of images is the geomechanical quality of local rocks, which is usually classified as "poor" and "very poor", which can also explain the low coherence (as shown in Fig. 5).

In the GIS environment, using ArcGIS software, the IPTA information and geomechanical map for N5E mine were compared in order to explore spatial relationships. Table 1 shows that the highest amount of PS was associated with the geomechanical classes of the largest areas, but not necessarily with the highest densities (class II). The highest density of points is class III (good rock), which is related to regions with less intense exploration activities. The regions with more intense exploration activities (classes IV and V)

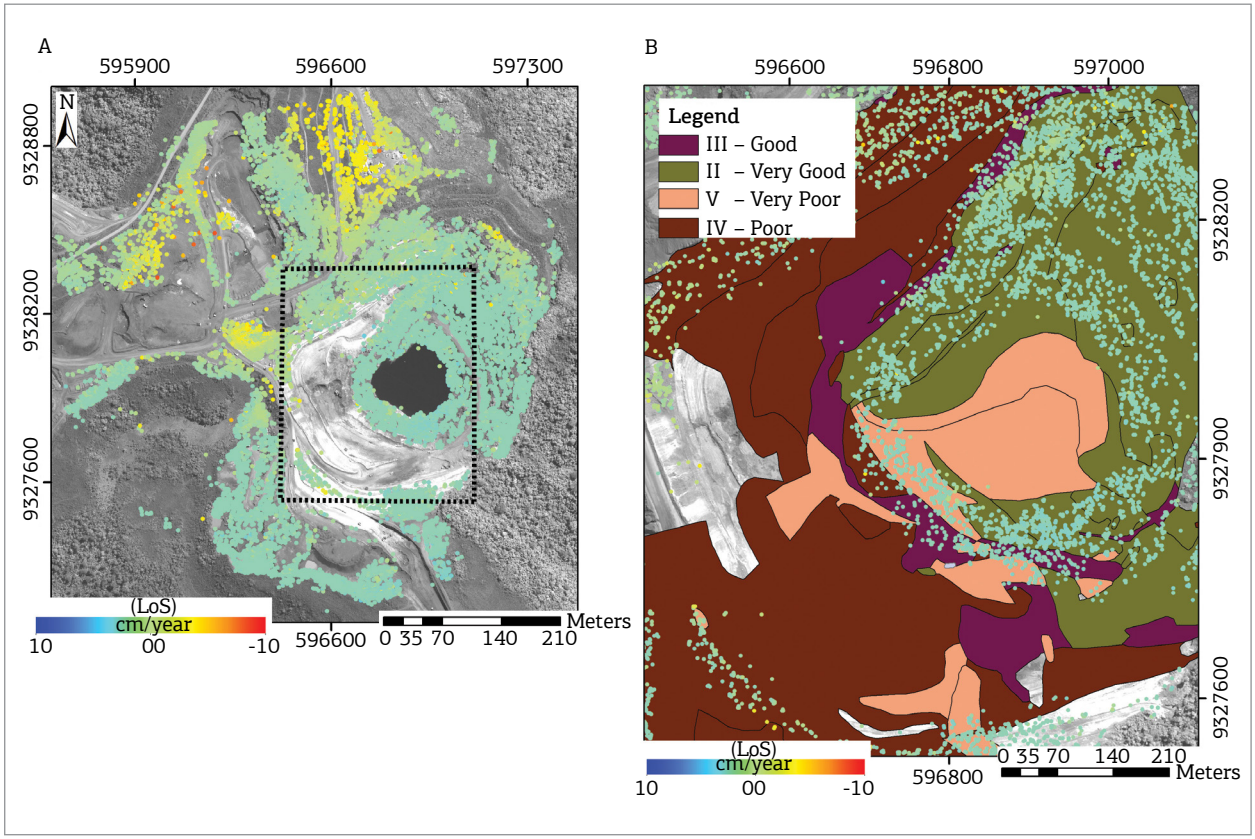


**Figure 5. (A) Spatial distribution of persistent scatterers (PSs) for N5E mine, visualized by the average line of sight (LoS) velocity on the panchromatic GeoEye-1 for the dry season; (B) geomechanical map under the PSs on the panchromatic GeoEye-1.**

presented lower density of points, both for the dry season and for the set of images of the wet season. This can be explained due to the fact these areas present a greater removal of material, causing a greater temporal uncorrelation between the images and, consequently, decreasing the interferometric coherence.

In an attempt to validate the differential SAR interferometry (DInSAR) time-series results restricted to the monitoring of the benches with field surface displacements, topographic measurements were also used. Geotechnical field measurements were available based on seven reflective prisms located on the east side of the benches (Fig. 6A, B). N5E mine is not commonly affected by intense mining activity as the remainder N4W, N4E and N5W mines. Therefore, the removal of material is done sporadically, so the extracted ore is blending with the material removed from other mines of the CMP. Due to this reason, the slopes of the eastern region present an apparent stability with greenish colors in the processing of IPTA, both for dry season and for rainy season.

In order to explore the relations of displacements and to validate the data generated by IPTA, two graphs (Fig. 7) were generated with the displacement data of the topographic measurement (total station and reflective prisms) and IPTA. Considering that measurements with satellite radar (TSX-1) and topographic data have different line of sight (LoS) monitoring, the prism vertical values were projected along the satellite LoS by multiplying these values by the cosine of the incidence angle. The field measurement chosen for the validation in this paper was referent to prism # 3 (Fig. 6B)

**Table 1. Relationship between persistent scatterers (PS) and geomechanical classes for N5E mine.**

| Geomechanical class | Area (km²) | Dry Season | | Wet Season | |
|---|---|---|---|---|---|
| | | Number of PSs | PS/km² | Number of PSs | PS/km² |
| III – Good rock | 0,07 | 3,386 | 48.371 | 3,384 | 48.342 |
| IV – Poor rock | 0,41 | 4,020 | 9.805 | 4,016 | 9.795 |
| V – Very poor rock | 0,19 | 1,171 | 6.163 | 1,169 | 6.152 |
| II – Very good rock | 0,23 | 2,836 | 12.330 | 2,835 | 12.326 |

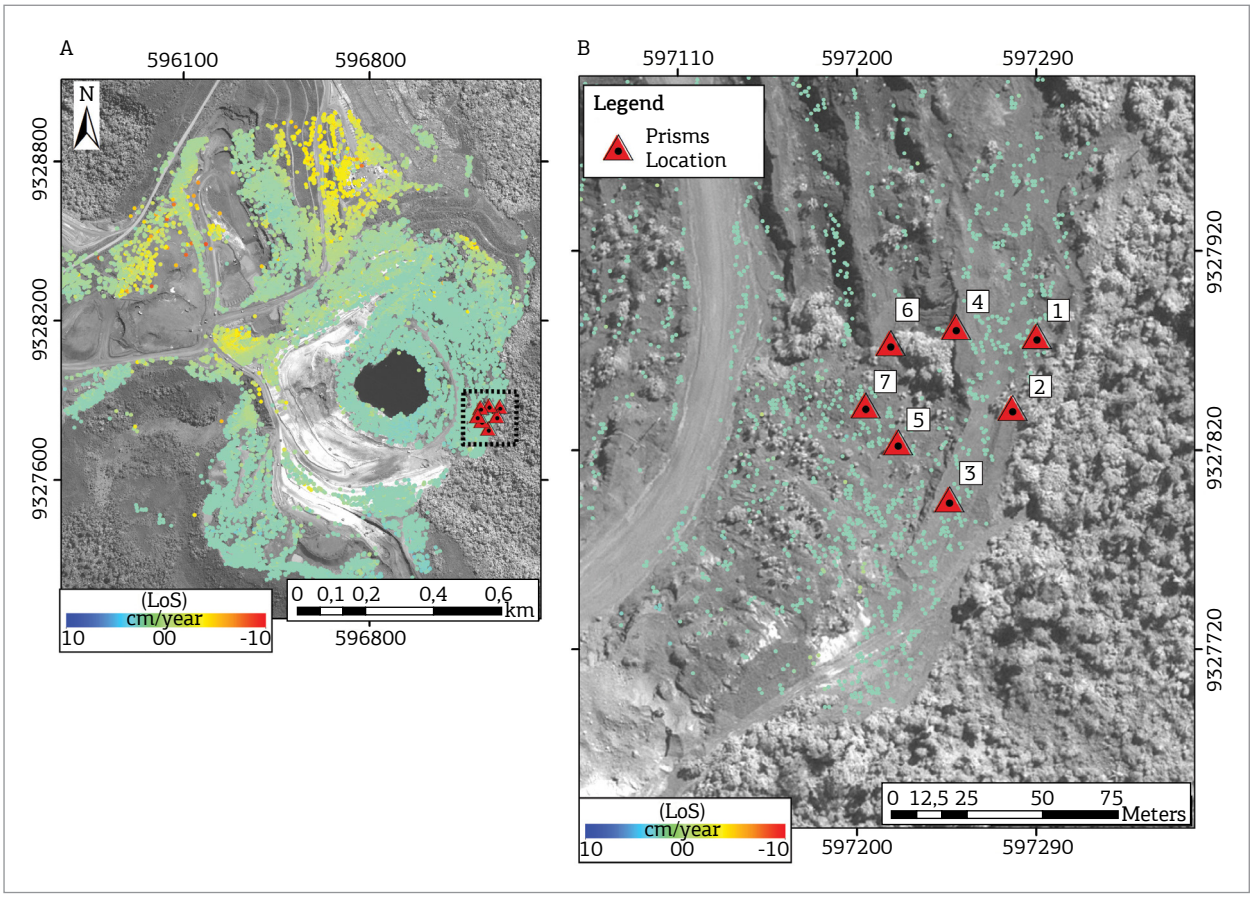


**Figure 6. (A) Spatial distribution of persistent scatterers (PSs) for N5E mine, visualized by the average line of sight (LoS) velocity on the panchromatic GeoEye-1 for the dry season; (B) seven prisms on the panchromatic GeoEye-1.**

and the correspondent PS was # 73143, both with the same geographical coordinates (597244,25E; 9327793,943N). The Vale S.A company that owns the mining right of the CMP defines as a safety threshold values of vertical displacement within +/- 2 cm for field measurement along the walls of the pit benches. That is, displacements greater than this threshold pose a risk for operation. The threshold was projected along the satellite LoS by multiplying these values by the cosine of the incidence angle, resulting in +/- 1,53 cm. The graphs show that, for both the dry season and the rainy season, the deformations on the surface measured by PS, during TSX-1 passage coverage, are within the miner's safety threshold and do not pose a risk of major problems. According to Vale's geotechnical team, the highest deformation value measured by the topographic surveying was -0.956 cm, which is considered a normal subsidence value for an active open pit.

This stability is due to the fact that N5E is not very active comparing with the other mines of the CMP (N5W, N4E, N4W), as was previously mentioned, mainly in the eastern portion of the pit, where the prisms were located, as shown in Figure 6B. The PS is located in a geologically mapped location as OD (Fig. 8), that covers iron ore and is formed by blocks of hematite (hard and semi-hard) cemented by hydrated oxides of iron. This type of rock is very hard, that is why it is normally expected there not to be large deformations on its surface. Unlike locations mapped as a landfill, which, as previously mentioned, is the lithology with the greatest deformations, due to the accommodation of material.


**Figure 7. Temporal evolution of the LoS-projected deformation for the PS # 731413, field displacements (prism # 3) covering dry and wet seasons and mining company security threshold.**

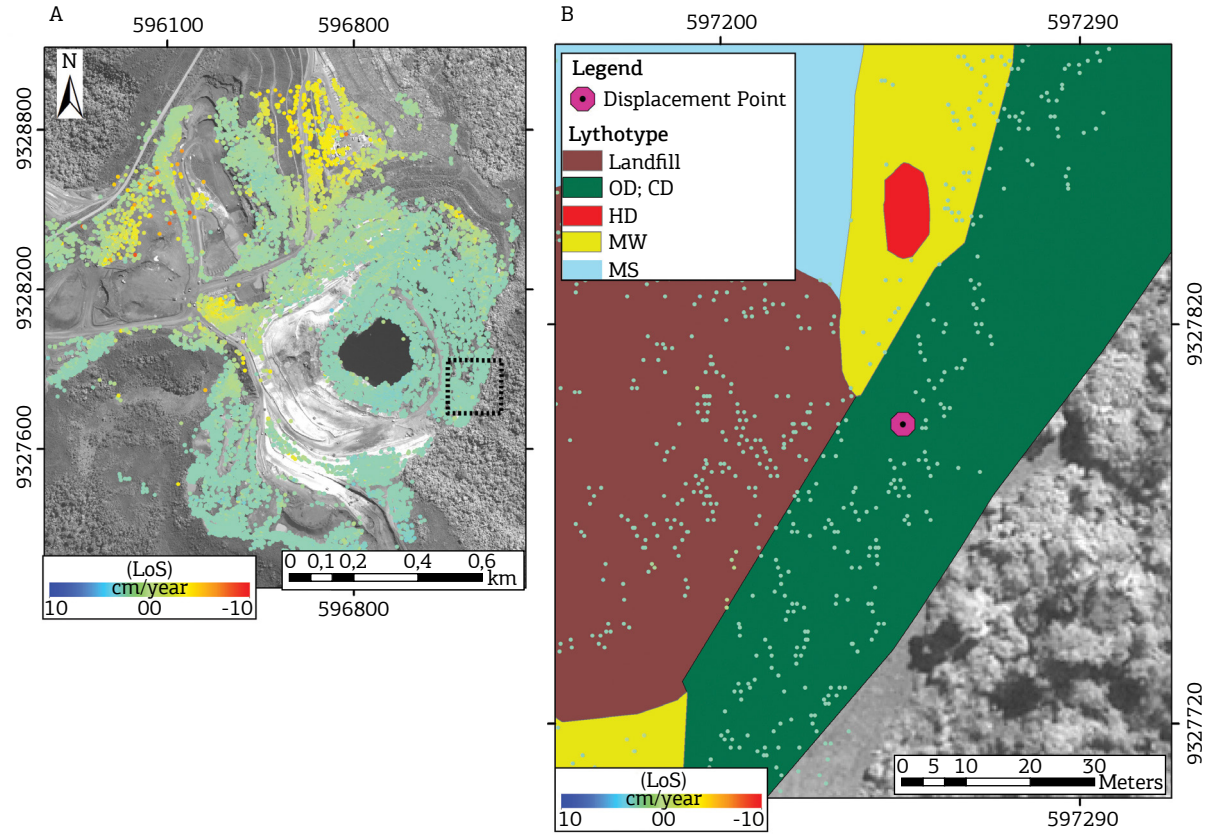


Acronyms: OD: ore duricrust; CD: chemical duricrust; HD: hard hematite; MW: mafic weathered; MS: mafic shan.

**Figure 8. (A) Spatial distribution of persistent scatterers (PS) for N5E mine, visualized by the average line of sight (LoS) velocity on the panchromatic GeoEye-1 for the dry season; (B) geological map under the PS on the panchromatic GeoEye-1.**

## CONCLUSIONS

The IPTA results showed that most of the mining area was stable during the TSX-1 coverage period, according the validation carried out using topographic surveying (total station and reflecting prisms).

The validation analysis during both dry and rainy season pointed out that the surface deformations during TSX-1 runway coverage are within the miner's safety threshold and do not present a risk of major problems.

The highest soil displacement values indicative of subsidence were measured in a landfill in the northern part of the pit and were interpreted as expected settlements, without additional evidence major terrain instability. The IPTA information and geomechanical map of the N5E mine were compared to explore spatial relationships. The highest density of points was related to Class III (good rock), which refers to less intense areas of exploitation activities. The region with more intense mining activities (Classes IV and V) presented lower density of points due to a decrease interferometric coherence.

The PSI data provided a synoptic and detailed view of the deformation process that affects the mining complex without the need of field campaign or instrumentation. The PSI approach, providing data with high displacement accuracy over a dense grid and large area, can be used for long-term operational monitoring planning and predictive solutions for mining operations and risk assessment. Since the space-based DInSAR information is not a real time approach, a complementary use of field monitoring systems is fundamental from an operational perspective.

## ACKNOWLEDGMENTS

The authors would like to thank São Paulo Research Foundation (FAPESP) (Grant # 2010/51267-9), and

the National Council for Scientific and Technological Development (CNPq) is also acknowledged for grants received by the first and fourth authors during this investigation. The authors are particularly grateful to the geotechnical Vale's team from Carajás, particularly geologist Aristotelina Silva, for the access of geological and geotechnical information, as well as to Dr. Maurício Galo (São Paulo State University "Júlio de Mesquita Filho" — UNESP, Presidente Prudente, Brazil) for helpful suggestions during topographic data analysis.

## REFERENCES

Beisiegel V.R., Bernardelli A.L., Drumond N.F., Ruff A.W., Tremaine J.W. 1973. Geology and Mineral Resources of Serra dos Carajás. *Brazilian Journal of Geosciences*, **3**:215-242.

Brito S. 2011. *The Slopes of Mining: Importance and Risks*. Workshop II: Geotechnics and Hydrogeology Applied to Mining. 14 Brazilian Congress of Mining.

BVP Engenharia. *Lithostructural and Lithogeomechanical Mapping of N5E Mine*. VL 070-10-E-CA-RT-03-102-00. Internal Vale Report. October 2011, 76 p.

Costantini F., Mouratidis A., Schiavon G., Sarti, F. 2016. Advanced InSAR techniques for deformation studies and for simulating the PS assisted calibration procedure of Sentinel-1 data: case study from Thessaloniki (Greece), based on the Envisat/ASAR archive. *International Journal of Remote Sensing*, **37**:729-744.

DNPM – National Department of Mineral Production. *Mineral Report*. Jan/Jun 2015.

Ferretti A., Prati C., Rocca F. 2000. Nonlinear Subsidence Rate Estimation Using Permanent Scatterers in Differential SAR Interferometry. *IEEE Transactions on Geoscience and Remote Sensing*, **38**:2202-2212. doi:10.1109/36.868878.

Ferretti A., Prati C., Rocca F. 2001. Permanent Scatterers in SAR Interferometry. *IEEE Transactions on Geoscience and Remote Sensing*, **39**:8-20. doi:10.1109/36.898661.

Gama F.F., Paradella W.R., Mura J.C., Santos A.R. 2013. Técnicas de interferometria radar na detecção de deformação superficial utilizando dados orbitais. *XVI Brazilian Symposium on Remote Sensing*. Foz do Iguaçu. v. 1. p. 8405-8812.

Ge L., Chang H., Rizos C. 2007. Mine subsidence monitoring using multi-source satellite SAR images. *Photogrammetric Engineering and Remote Sensing*, **73**:259-266.

Holdsworth R., Pinheiro R.V.L. 2000. The anatomy of shallow-crustal transpressional structures: insights from the Archean Carajás Fault Zone, Amazon, Brazil. *Journal of Structural Geology*, **22**:1105-1123.

Hooper A., Zebker H., Segall P., Kampes B. 2004. A New Method for Measuring Deformation on Volcanoes and Other Natural Terrains Using Insar Persistent Scatterers. *Geophys Researcher Letters*, **31**:1-5. doi: 10.1029/2004GL021737.

Meireles E.M., Hirata W.K., Amaral A.F., Medeiros Filho C.A., Gato W.C. 1984. Geology of Carajás and Rio Verde Folios, Carajás Mineral Province, State of Pará. 33 *Brazilian Congress of Geology*. Rio de Janeiro, p. 2164-2174.

Ng A.H.M., Chang H.C., Ge L., Rizos C., Omura M. 2009. Assessment of radar interferometry performance for ground subsidence monitoring due to underground mining. *Earths, Planets and Space*, **61**:733-745.

Ng A.H.M, Ge L., Zhang K., Chang H.C., Li X., Rizos C., Omura, N. 2011. Deformation mapping in three dimensions for underground mining using InSAR – Southern highland coalfield in New South Wales, Australia. *International Journal of Remote Sensing*, **22**:7227-7256. doi: 10.1080/01431161.2010.519741

Paradella W.R., Cheng P. 2013. Using GeoEye-1 Stereo Data in Mining Applications: Automatic DEM Generation. *Geoinformatics*, **16**:10-12.

Paradella W.R., Ferretti A., Mura J.C., Colombo D., Gama F.F., Tamburini A., Santos A.R. 2015. Mapping surface deformation in open pit iron mines of Carajás Province (Amazon Region) using an integrated SAR analysis. *Engineering Geology*, **193**:61-78.

Paradella W.R., Silva M.F.F., Rosa N.A., Kushigbor C.A. 1994. A geobotanical approach to the tropical rain forest environment of the Carajás Mineral Province (Amazon region, Brazil) based on digital TM-Landsat and DEM data. *International Journal of Remote Sensing*, **15**:1633-1648.

Pinto C.A., Paradella W.R., Mura J.C., Gama F.F., Santos A.R., Silva G.G., Hartwig M.E. 2015. Applying persistent scatterer interferometry for surface displacement mapping in the Azul open pit manganese mine (Amazon region) with TerraSAR-X StripMap data. *Journal of Applied Remote Sensing*, **9**:095978-1-095978-18. doi: 10.1117/1.JRS.9.095978.

Stacey P., Read J. 2009. *Guidelines for Open Pit Slop Design*. CSIRO publishing, Australia.

Vaziri A., Moore L., Ali H. 2010. Monitoring systems for warning impending failures in slopes and open pit mines. *Natural Hazards*, **55**:510-512.

Veneziani P., Santos A.R., Paradella W.R. 2004. A evolução tectono-estratigráfica da Província Mineral de Carajás: um modelo com base em dados de sensores remotos orbitais (SAR-C RADARSAT-1, TM LANDSAT-5), aerogeofísica e dados de campo. *Brazilian Journal of Geoscience*, **34**:67-78.

Werner C., Wegmuller U., Strozzi T., Wiesmann A. 2003. Interferometric point target analysis for deformation mapping. IEEE Geoscience and Remote Sensing Symposium. *Toulouse*, **7**:4362-4364.

Zebker H.A., Villasenor J. 1992. Decorrelation in interferometric radar echoes. *IEEE Transactions on Geoscience and Remote Sensing*, **30**:950-959.